

Solvothermal Depolymerization and Recrystallization of Imine-Linked Two-Dimensional Covalent Organic Frameworks

Woojung Ji¹, Leslie S. Hamachi^{1,3}, Anusree Natraj¹, Nathan Flanders¹, Rebecca L. Li¹, Lin X. Chen^{1,2},
and William R. Dichtel^{1,*}

¹ *Department of Chemistry, Northwestern University,
2145 Sheridan Road, Evanston, Illinois 60208, United States*

² *Chemical Sciences and Engineering Division, Argonne National Laboratory,
Argonne, Illinois 60439, United States*

³ *Department of Chemistry and Biochemistry, California Polytechnic State University, San Luis Obispo,
California, 93407, United States*

Supplementary Information

Correspondence Address
Professor William R. Dichtel Department of Chemistry Northwestern University 2145 Sheridan Road Evanston, IL 60208 (USA) wdichtel@northwestern.edu

Table of Contents

A. Materials and Instrumentation	S-2
B. Synthetic Procedures	S-5
C. Additional Images and Characterization	S-6
D. BET Plots for N ₂ Isotherm	S-13

A. Materials and Instrumentation.

Materials. Reagents were purchased in reagent grade from commercial suppliers and used without further purification, unless otherwise described. Borosilicate capillaries (1.5 mm in diameter and a wall thickness of 0.01 mm) were purchased from Charles Supper.

Instrumentation. Infrared spectra were recorded using a Nicolet iS10 FT-IR spectrometer equipped with a ZnSe ATR.

Variable temperature proton nuclear magnetic resonance (VT-¹H NMR) spectra were recorded on Bruker AvanceIII-600 MHz.

The supercritical CO₂ drying was performed on Leica EM CPD 300. Prior to the supercritical drying process, all samples were placed in tea bags (ETS Drawstring Tea Filters, sold by English Tea Store) while wet. The tea bags containing the samples were then placed in the drying chamber. The drying chamber was first sealed, cooled, and filled with liquid CO₂, and after 2 min, the samples were vented quickly. This fill-vent cycle was repeated 99 times, after which the temperature was raised to 40 °C resulting in a chamber pressure of around 1300 psi, which is well above the critical point of CO₂. The chamber was held above the critical point for 5 min, after which the CO₂ source was turned off, and the pressure was released over a period of 5 min.

Powder X-ray diffraction (PXRD) patterns were obtained at room temperature on a STOE-STADIMP powder diffractometer equipped with an asymmetric curved Germanium monochromator (CuK α ₁ radiation, $\lambda = 1.54056 \text{ \AA}$) and one-dimensional silicon strip detector (MYTHEN2 1K from DECTRIS). The line focused Cu X-ray tube was operated at 40 kV and 40 mA. The as-obtained powder samples were sandwiched between two acetate foils (polymer sample with neither Bragg reflections nor broad peaks above 10° 2 θ) mounted in flat plates with a disc

opening diameter of 8 mm and measured in transmission geometry in a rotating holder. The patterns were recorded in the 2θ range of 0–32° for an overall exposure time of 24 min. The instrument was calibrated against a NIST Silicon standard (640d) prior to the measurement.

Wide-angle X ray scattering (WAXS) patterns were collected at sector 5-ID-D of the Advanced Photon Source at Argonne National Lab. A beam energy 13.3 keV was used at 5-ID-D. Each pattern was obtained by collecting ten one second frames on a Pilatus 2D detector and then averaged and radially integrated using software available at APS.

Gas adsorption isotherms were conducted on a Micromeritics ASAP 2420 Accelerated Surface Area and Porosity Analyzer using 15–50 mg samples in dried and tared analysis tubes equipped with filler rods and capped with a Transeal. Samples were heated to 40 °C at a rate of 1 °C/min and evacuated at 40 °C for 20 min, then heated to 100 °C at a rate of 1 °C/min heat and evacuated at 100 °C for 18 h. After degassing, each tube was weighed again to determine the mass of the activated sample and transferred to the analysis port of the instrument. UHP-grade (99.999% purity) N₂ was used for all adsorption measurements. N₂ isotherms were generated by incremental exposure to nitrogen up to 760 mmHg (1 atm) in a liquid nitrogen (77 K) bath. Oil-free vacuum pumps and oil-free pressure regulators were used for all measurements. Brunauer-Emmett-Teller (BET) surface areas were calculated from the linear region of the N₂ isotherm at 77 K within the pressure range P/P_0 of 0.10–0.20.

Scanning electron microscopy (SEM) images of TAPB-PDA and TAPB-DMTA COFs samples were taken on a Hitachi S4800 cFEG SEM. The samples were coated with 8 nm of Osmium using SPI OPC-60A osmium plasma coater.

Dynamic light scattering (DLS) experiments were conducted using a Malvern Zetasizer with a 633 nm HeNe 5mW laser at different temperatures with 10 mm pathlength quartz cuvette. The data was analyzed using the Zetasizer software.

B. Synthetic Procedures

COF Synthesis at Room Temperature: A 20 mL scintillation vial was charged with benzoic acid (675 mg, 5.5 mmol) and corresponding aldehyde (0.072 mmol of **PDA** or **DMTA**) in benzonitrile (6 mL) and heated to 90 °C for a few minutes to ensure dissolution of each species. The solution was cooled to room temperature and water (0.375 mL, 21 mmol), aniline (0.1 mL of 0.7 M stock in benzonitrile, 0.07 mmol), and 1,3,5-tris(4-aminophenyl)benzene (**TAPB**, 17 mg, 0.048 mmol) were added. The resulting reaction mixture was let stand at room temperature for 3 hours until it turned opaque to serve as room temperature synthesized COF colloids. These COFs were then precipitated out by the addition of 0.2 mL brine and 10 mL methanol, centrifuged for 10 minutes, transferred to a tea bag, and washed with methanol in a Soxhlet extractor for 18 h. The materials were activated by supercritical CO₂ that afforded COFs as yellow solids in isolated yields of 75%.

COF Recrystallization: COF colloids in their original reaction mixtures were used right after their 3-hour reaction at room temperature. These solutions were heated to 90 °C for 3 hours, after which the solution was observed to turn clear red. The COF solution was then cooled to room temperature and let sit for 18 hours to be transferred to a tea bag, and washed with methanol in a Soxhlet extractor for 18 h. The materials were activated by supercritical CO₂ that afforded **Recrystallized COFs** as yellow solids in isolated yields of 85%.

C. Additional Images and Characterization

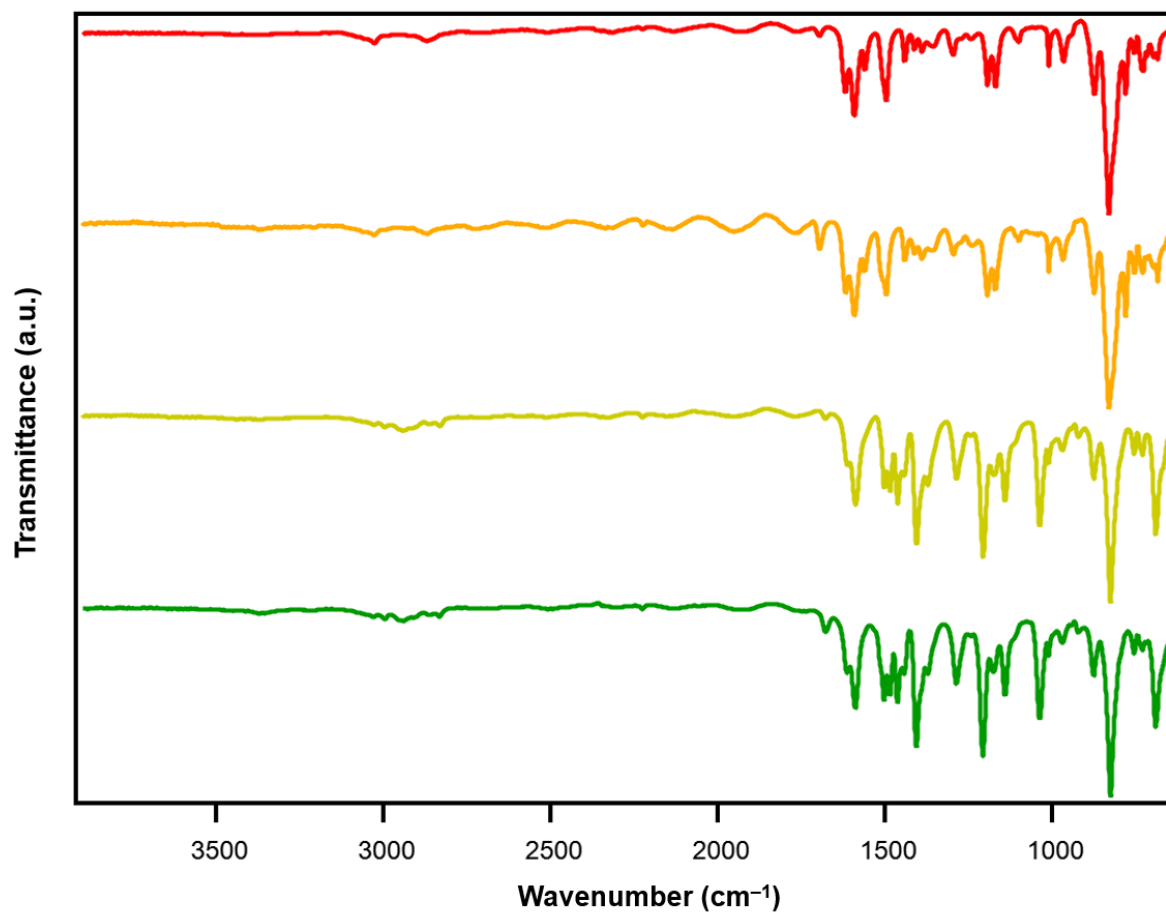


Figure S1. FT-IR Spectra of colloidal (red) and recrystallized (orange) **TAPB-PDA COF**, and colloidal (yellow) and recrystallized (green) **TAPB-DMTA COF**.

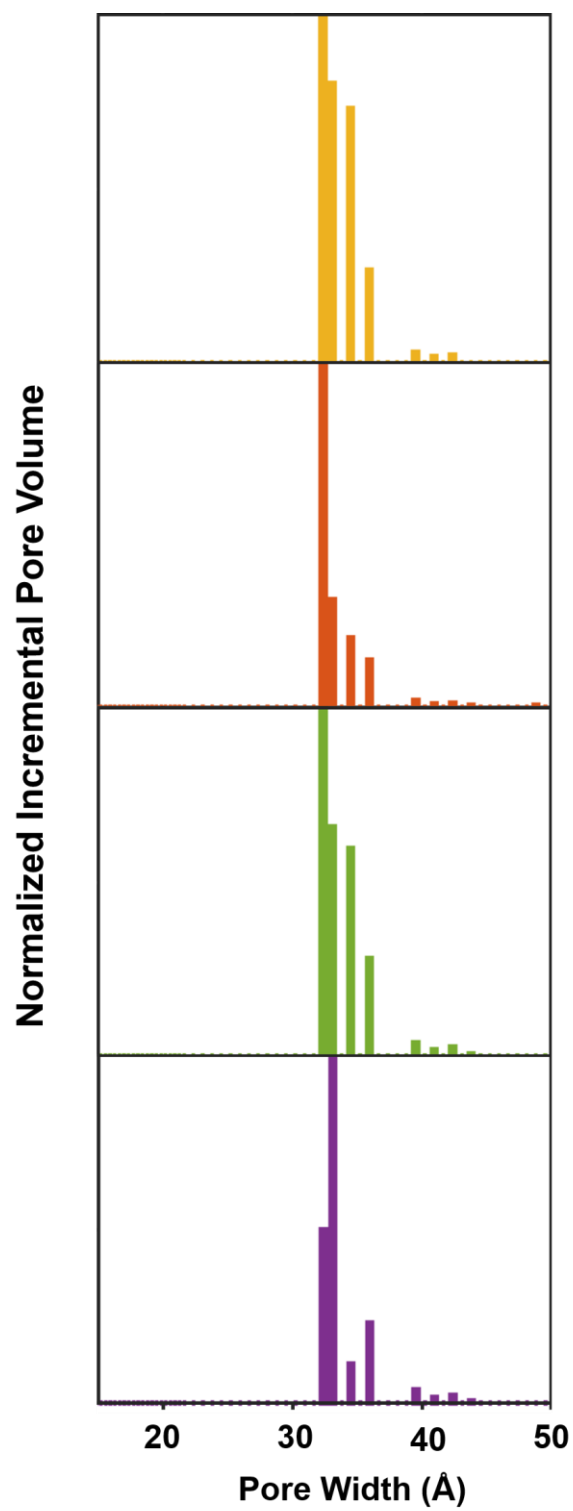


Figure S2. Pore size distributions of colloidal (yellow) and recrystallized (red) **TAPB-PDA COF**, and colloidal (green) and recrystallized (purple) **TAPB-DMTA COF**.

Representative NMR Spectrum

Bruker Avance III 600 MHz

90 °C in benzonitrile- d_5

Internal Standard: 1,4- Dinitrobenzene

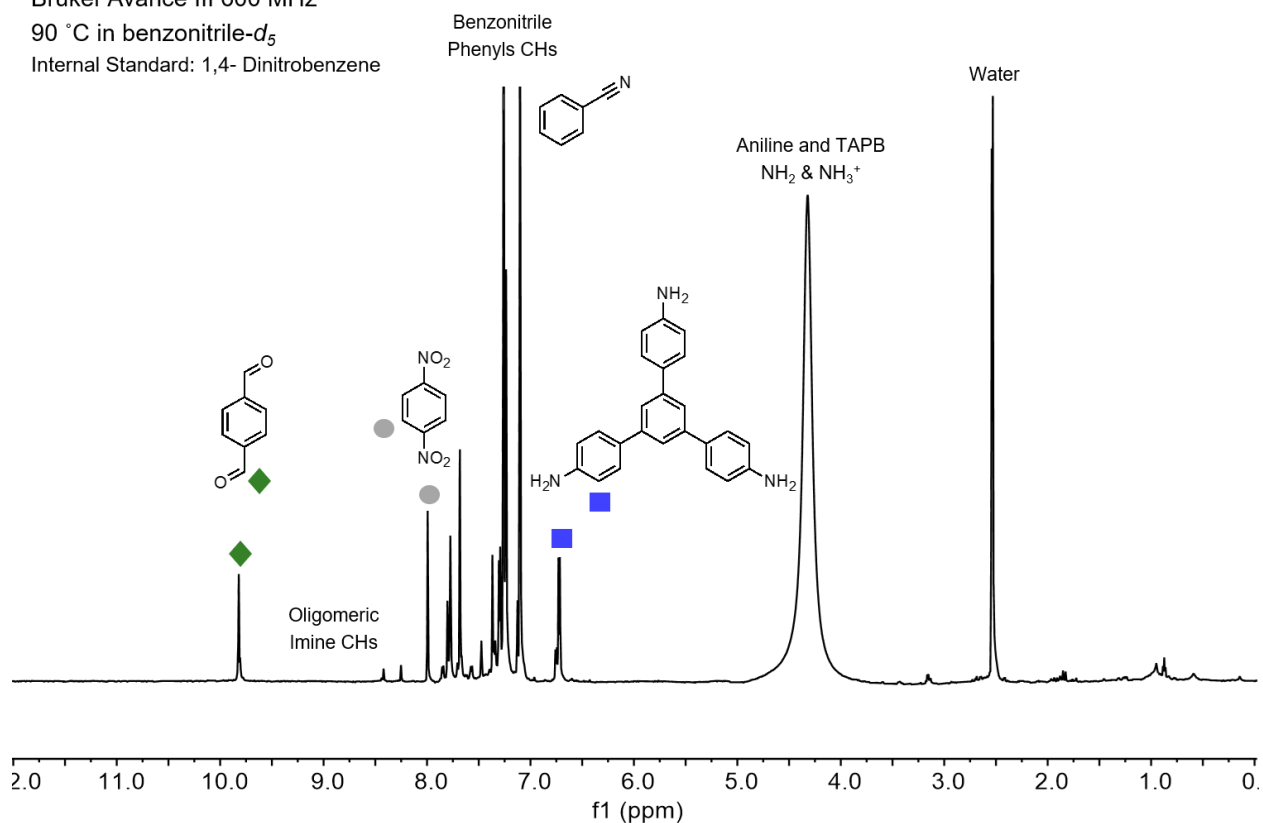


Figure S3. Representative VT-NMR spectrum (0–12 ppm) of **TAPB-PDA COF** reaction mixture at 90 °C in benzonitrile- d_5 .

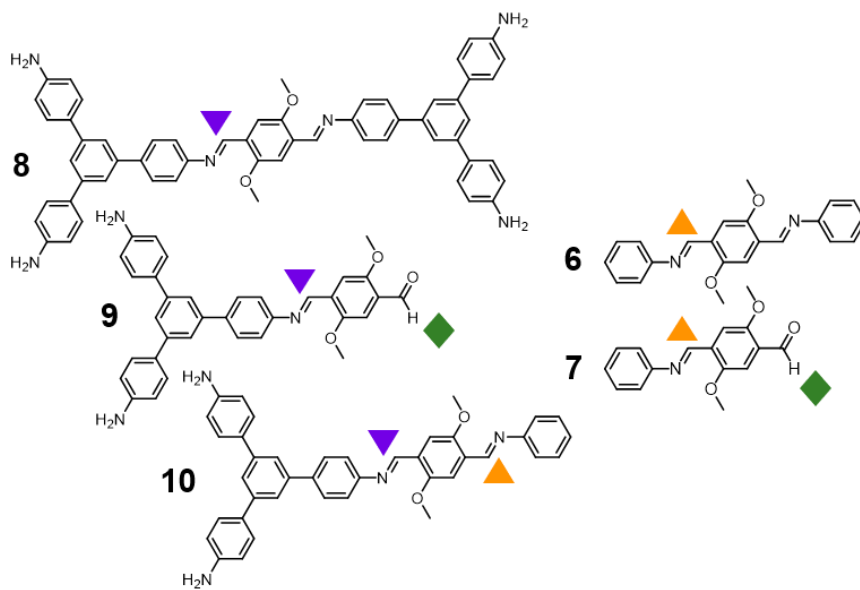


Figure S4. Soluble imine-linked species in the representative VT-NMR spectrum in **Figure 7a**.

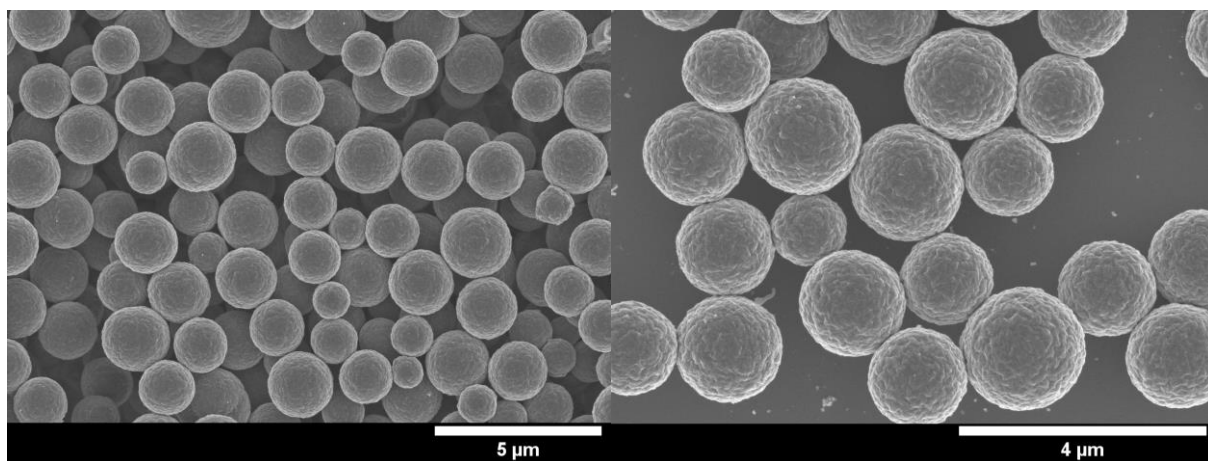


Figure S5. SEM images of colloidal TAPB-PDA COFs.

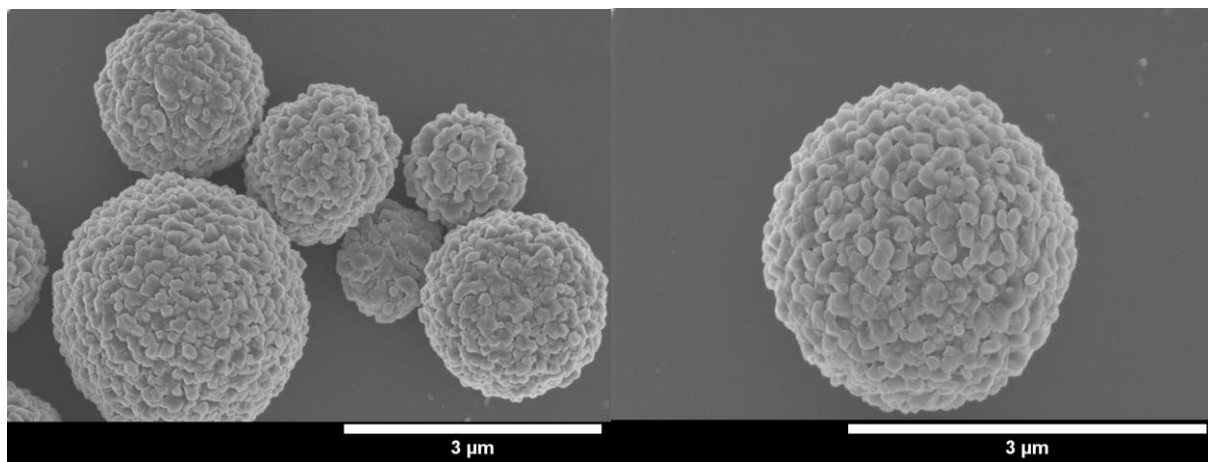


Figure S6. SEM images of colloidal TAPB-DMTA COFs.

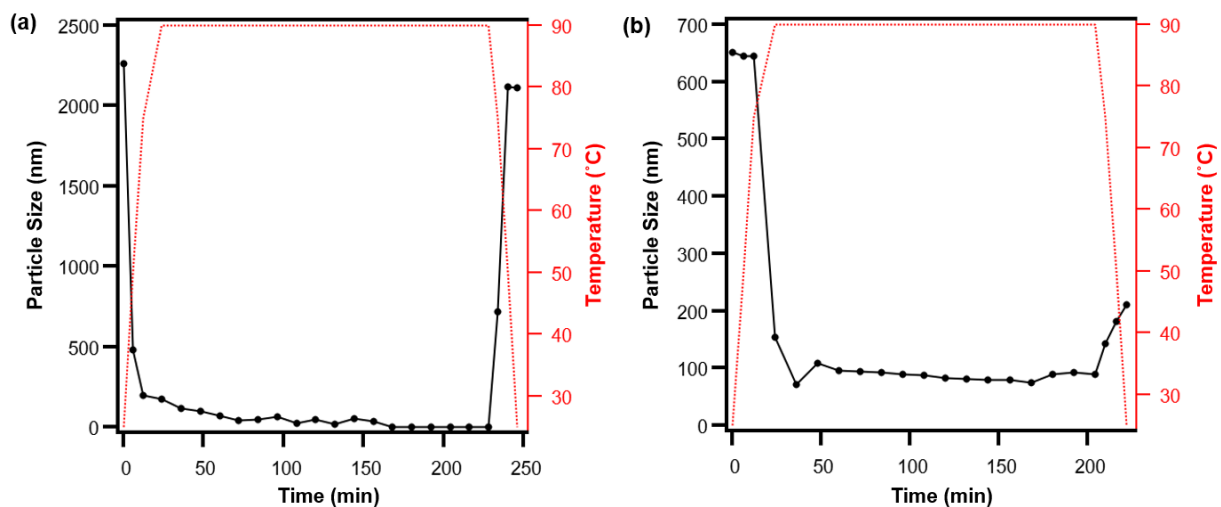


Figure S7. Change in average particle sizes of (a) **TAPB-PDA COF** and (b) **TAPB-DMTA COF** during the first cycle of COF recrystallization, as determined by DLS experiments.

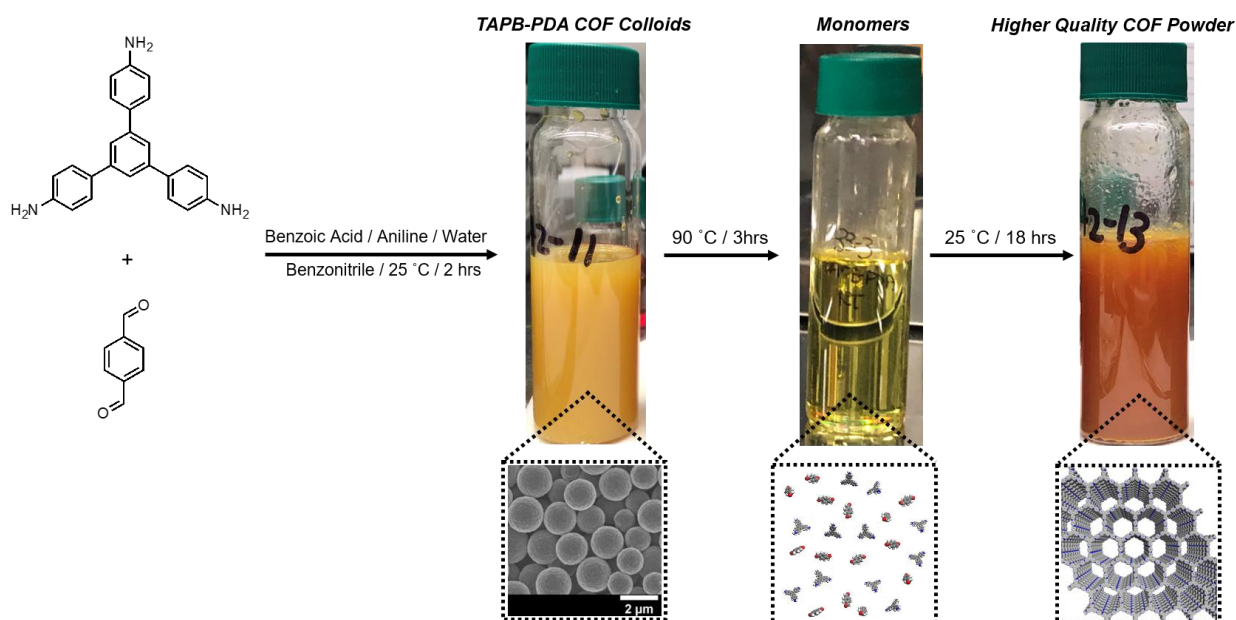


Figure S8. Schematic of **TAPB-PDA COF** recrystallization with pictures.

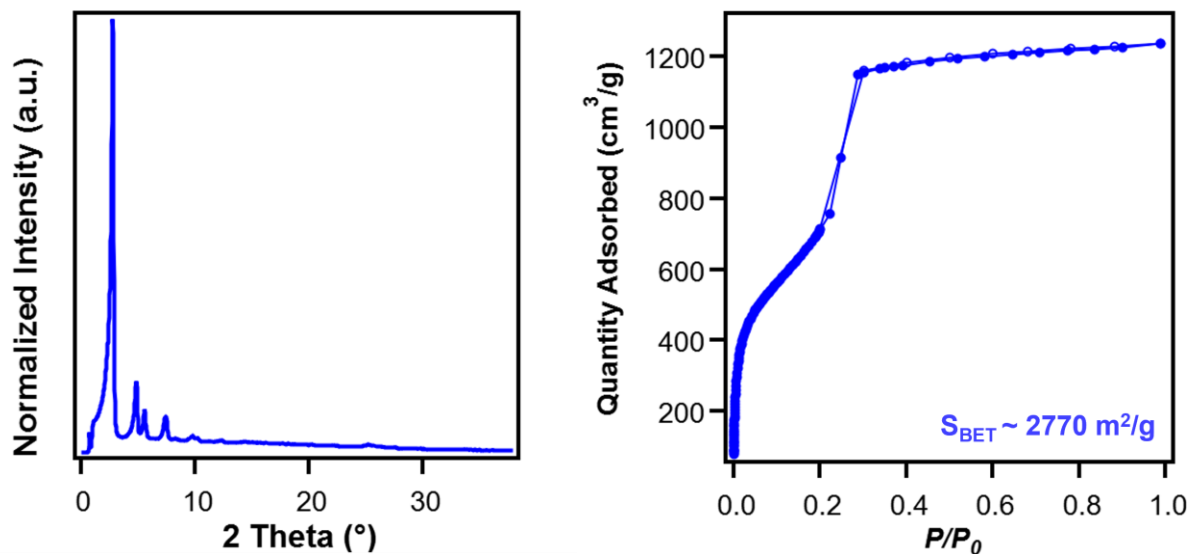


Figure S9. PXRD pattern and N₂ adsorption isotherm of TAPB-PDA COF after which separate solutions of the two monomers were heated to 90 °C, combined, and cooled to induce COF formation.

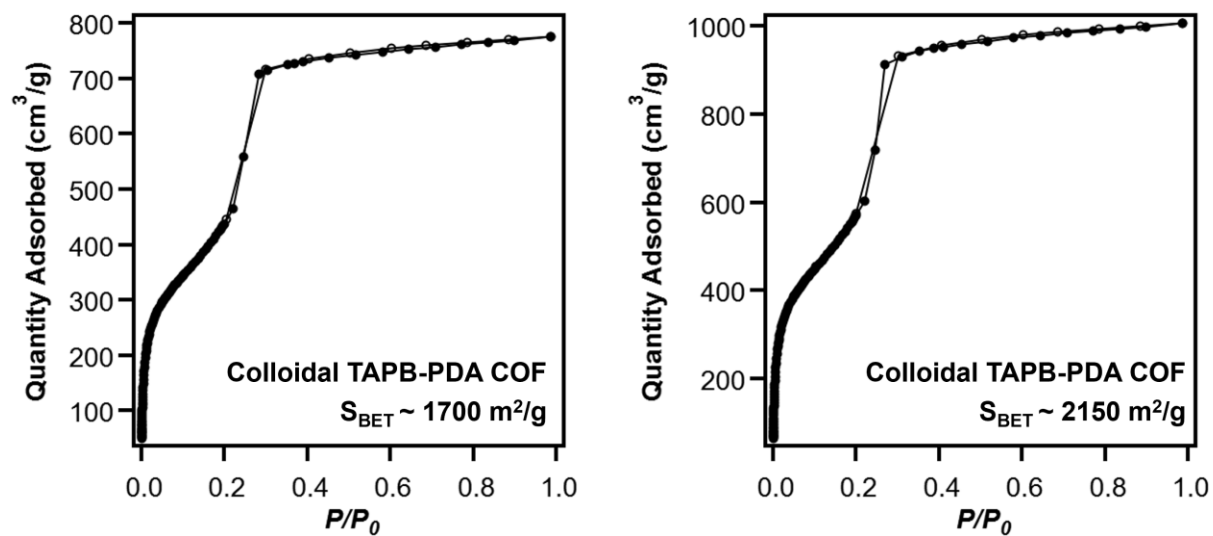


Figure S10. Additional N₂ adsorption isotherms of colloidal TAPB-PDA COFs.

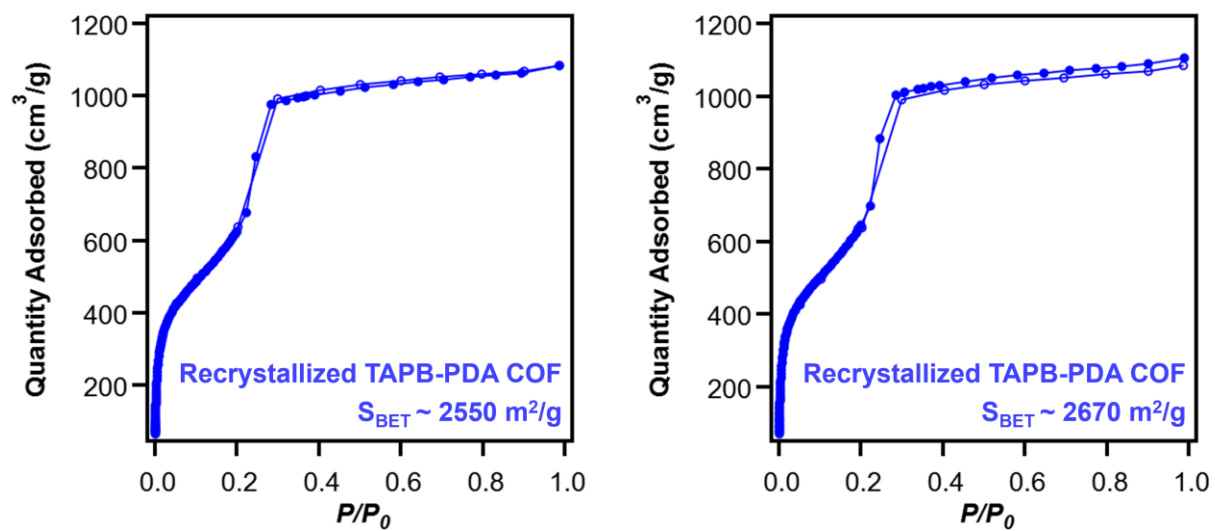


Figure S11. Additional N₂ adsorption isotherms of recrystallized TAPB-PDA COFs.

D. BET Plots for N₂ Isotherm

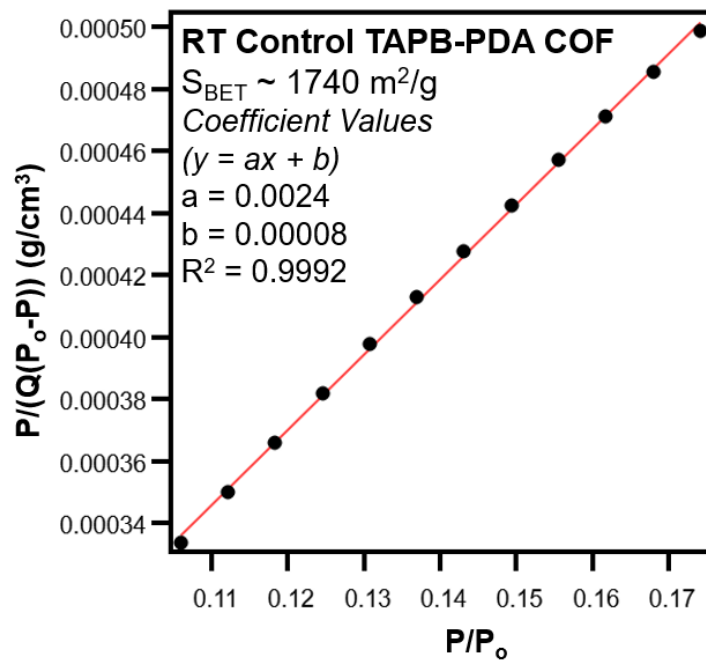


Figure S12. BET Plot for colloidal TAPB-PDA COF.

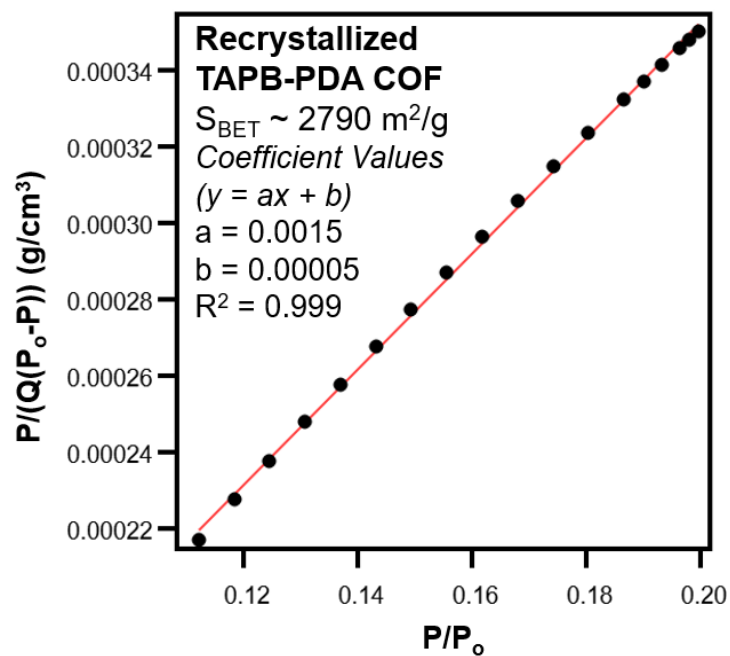


Figure S13. BET Plots for recrystallized TAPB-PDA COF.

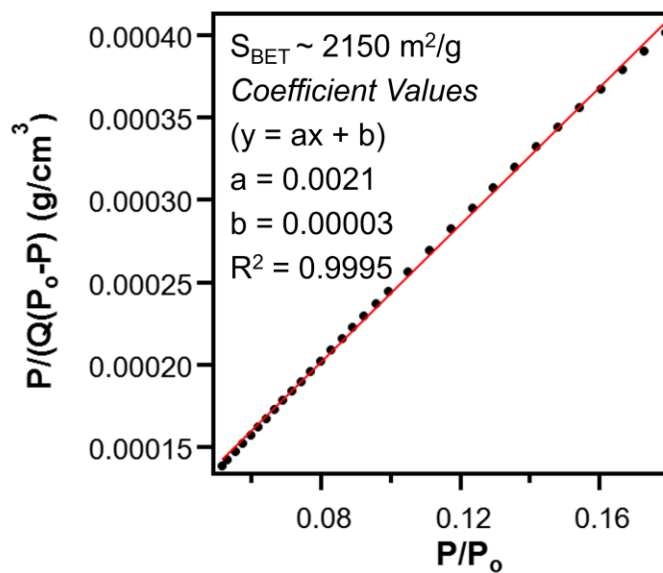
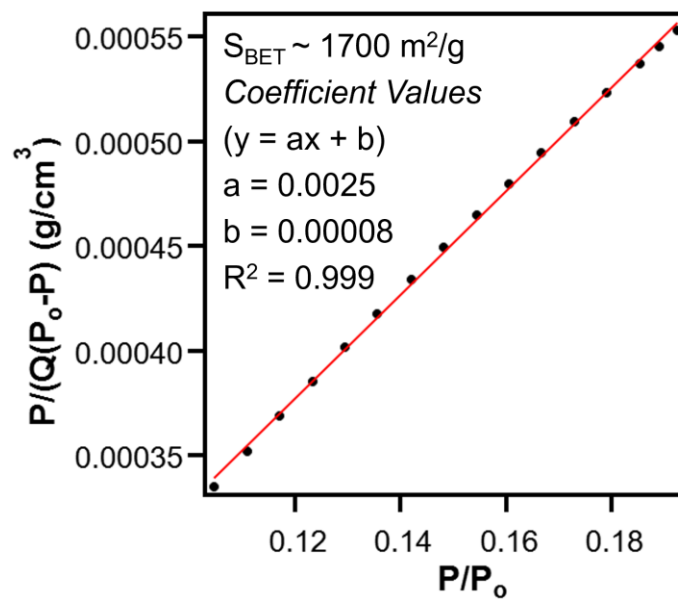


Figure S14. Additional BET Plot for colloidal TAPB-PDA COF.

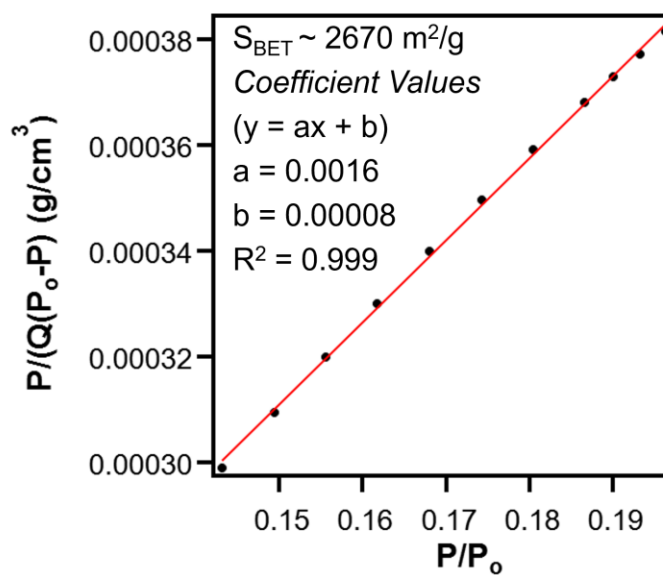
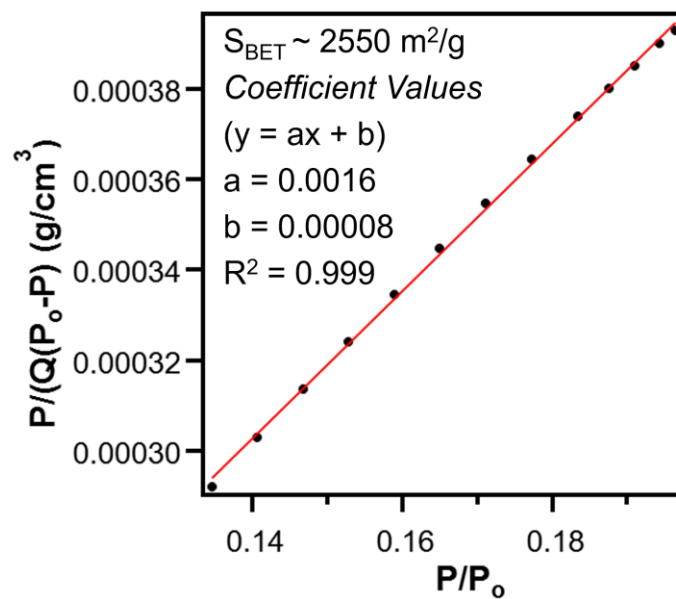


Figure S15. Additional BET Plots for recrystallized TAPB-PDA COF.

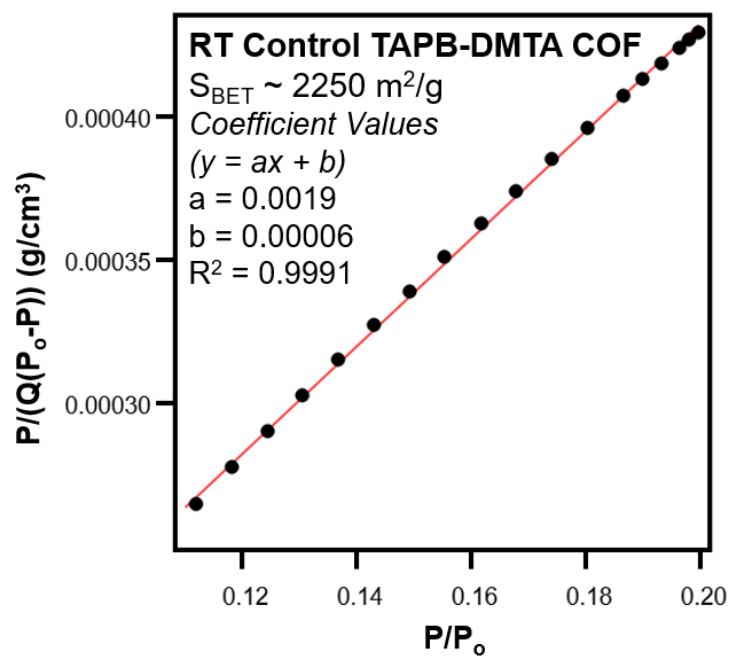


Figure S16. BET Plot for colloidal TAPB-DMTA COF.

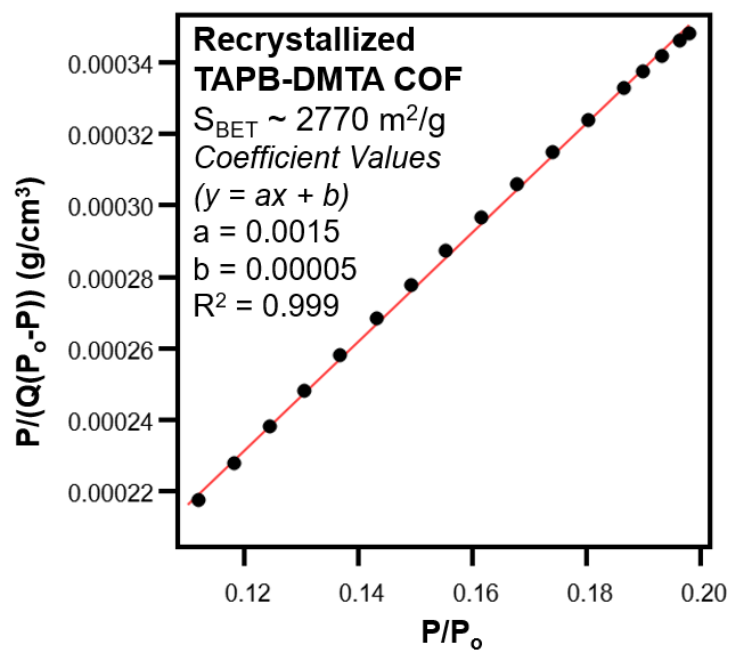


Figure S17. BET Plot for recrystallized TAPB-DMTA COF.